Ranges and Range Straggling of Tb^{149}, At, and Po†

LESTER WINSBERG AND JOHN M. ALEXANDER

Lawrence Radiation Laboratory, University of California, Berkeley, California

(Received September 15, 1960)

We report on ranges and range straggling of recoils from nuclear reactions induced by the ions C^{12}, N^{14}, O^{16}, O^{18}, and Ne^{22} with kinetic energies of 10 Mev per nucleon and less. Range-energy curves were obtained for Tb^{149} (recoil energies of 4 to 29 Mev) in Al, for At and Po (4 to 15 Mev) in Al, and for At and Po (4 to 9 Mev) in Au. Ranges of Tb^{149} at the threshold of each reaction were obtained by extrapolation. The agreement of these and the directly measured values supports the assumption of compound-nucleus formation used in calculating the recoil energies. The smaller recoil velocities in this study are of the same order as the Bohr velocity (2.2×10^8 cm/sec). The values of the average range and the straggling parameter are compared with stopping theory. The contribution to the measured range straggling from the nuclear reaction is discussed. Our results and the work of others are used to obtain values of the range for Xe^{139} in Al from 0.1 to 70 Mev and for At^{203} in Au from 0.01 to 10 Mev.

I. INTRODUCTION

INFORMATION concerning the stopping of atoms is fragmentary. The theoretical framework has been summarized by Bohr.[1] According to the theory, the nature of the stopping process is dependent on the velocity of the moving atom. If the velocity is greater than the orbital velocities of all electrons, the energy loss is mainly by interaction with the electrons of the stopping medium. In general, the experimental measurements bear out the theoretical predictions.[2]

For slow-moving atoms that have velocities less than the orbital-electron velocities, the energy loss is mainly by interaction with the atomic systems of the stopping medium. Theoretical equations have been given for range and range straggling of slow-moving atoms much heavier and much lighter than the stopping atoms.[1,3,4] The experimental tests of these equations, however, are few indeed. The range measurements that have been made agree with the theoretical equations within a factor of about two.[4–10] Some measurements of the range straggling are consistent with the theoretical equations, whereas others are not.[6–8]

No theoretical treatment is reported for slow-moving atoms similar in mass to the stopping atoms. However, a few range measurements have been reported.[6,7,9,10]

Qualitative theoretical treatments of stopping phenomena have been presented for atoms moving with velocities comparable to orbital-electron velocities.[1] Some experimental information is available from studies of fission fragments, but correlations of these data are still only empirical.[11]

We have made measurements of ranges and range straggling of recoils from nuclear reactions induced by the ions C^{12}, N^{14}, O^{16}, O^{18}, Ne^{20}, and Ne^{22}, with kinetic energies of 10 Mev per nucleon and less. The velocities of the recoiling atoms were comparable to orbital-electron velocities. Recoiling atoms of Tb, At, and Po were stopped in Al, which has much smaller mass than the recoils. The stopping of At and Po recoils in Au and Pt targets was also studied. In this case the recoil and stopping atoms have nearly equal mass.

The objectives of this work are twofold: (a) to extend our knowledge of the stopping process, and (b) to study the nature of nuclear reactions. In this paper we emphasize the study of stopping phenomena. In the following paper we concentrate on the study of nuclear-reaction mechanisms.[12]

II. EXPERIMENTAL PROCEDURE

We have performed three types of experiments: first, differential experiments in which the recoiling atoms from a thin target were stopped in thin catcher foils; second, integral experiments in which the total recoil loss from a thick target was observed; and third, experiments of the latter type but with the recoils from a thick target being caught in thin catcher foils. The recoil atoms were formed by nuclear reactions induced by heavy ions from the Berkeley heavy-ion linear accelerator. The nuclear-reaction products, Tb^{149} and several isotopes of At and Po, were observed by meas-

† This work was performed under the auspices of the U. S. Atomic Energy Commission.

[1] N. Bohr, Kgl. Danske. Videnskab. Selskab, Mat.-fys. Medd. 18, No. 8 (1948).

[2] R. D. Evans, *The Atomic Nucleus* (McGraw-Hill Book Company, Inc., New York, 1955), pp. 567, 632.

[3] J. Lindhard and M. Scharff (private communication quoted by Leachman and Atterling, see reference 8).

[4] K. O. Nielson, *Electromagnetically Enriched Isotopes and Mass Spectrometry* (Academic Press, Inc., New York, and Butterworths Scientific Publications, Ltd., London, 1956).

[5] D. L. Baulch and J. F. Duncan, Australian J. Chem. 10, 112 (1957). See this paper for a survey of other measurements.

[6] S. G. Cohen, *Proceedings of the Rehovoth Conference on Nuclear Structure*, edited by H. J. Lipkin (North-Holland Publishing Company, Amsterdam, 1958), p. 580.

[7] E. W. Valyocsik, Lawrence Radiation Laboratory Report UCRL–8855, November, 1959 (unpublished).

[8] R. B. Leachman and H. Atterling, Arkiv Fysik 13, 101 (1957).

[9] R. A. Schmitt and R. A. Sharp, Phys. Rev. Letters 1, 12, 445 (1958).

[10] B. G. Harvey, W. H. Wade, and P. F. Donovan, Phys. Rev. 119, 225 (1960).

[11] J. M. Alexander and M. F. Gazdik, Phys. Rev. 120, 874 (1960). Other references given here.

[12] John M. Alexander and Lester Winsberg, following paper [Phys. Rev. 121, 529 (1961)].

urements of the α radioactivity in the various foils. Targets of compounds of the elements Cs to Pr, were irradiated with heavy ions (HI) to form Tb¹⁴⁹ from (HI,xn) and (HI,pxn) reactions. Similar reactions with Au, Pt, Ir, and Re were employed in order to form At and Po nuclides.

The targets were thin layers evaporated onto 0.00025-inch Al by Dan O'Connell of this Laboratory. The substances used were $CsNO_3$, $BaCl_2$, La_2O_3, Ce, CeO_2, Pr_2O_3, Ir, Au, and Re. For differential experiments the target-layer thickness was 10 to 78 $\mu g/cm^2$. For integral experiments the target thicknesses were 0.3 to 6 mg/cm^2. In the Pt experiments commercial foils with thicknesses about 6 mg/cm^2 were used.

Catcher foils of commercially available Al were used. Spectroscopic analysis of the foils revealed the presence of 0.3% Fe and 0.1% Cu. Rolled foils of about 0.00025 inch thickness were used for the integral experiments. For the differential measurements Al leaf was used. The average thickness of each recoil catcher was obtained by area and weight measurements. Small squares (3.7 cm^2) cut from a given sheet of Al leaf (200 cm^2) varied gradually in average thickness from about 0.20 mg/cm^2 near the center to about 0.14 mg/cm^2 near the edge. In order to minimize the error in the thickness measurement we cut each catcher foil only slightly larger in area than the beam collimator. We did not measure the uniformity of the foils on a microscopic scale.

Stacked foils (20 to 150 in number) were clamped to a water-cooled copper holder and were irradiated for several hours with an average beam current of less than 0.1 μa. In order to check on the possibility of thermal diffusion we exposed two very similar foil stacks with Bi as the target to C^{12} beams of very different intensity. The results of the two irradiations (one with an average beam current of 0.05 μa and the other 0.3 μa) were

completely consistent. Therefore, we believe that any error due to diffusion is negligible.

Measurement of the α radiation of the foils was made with about 8 to 14 ionization chambers designed in this Laboratory for detecting fission, alpha, and beta pulses. The background counting rates were 0.2 to 1.0 count per minute. The gain of the counters was adjusted to obtain almost equal counting efficiency for a thick uranium standard. For the integral experiments, the relative activities were determined by simultaneous counting of the two or three samples of each set in rotating fashion. For the differential measurements a larger number of separate foils were counted in a nearly simultaneous fashion. The counting was repeated on different counters. Complete rotation of the samples was not usually possible, but the analysis of these experiments does not require as accurate counting as do the integral experiments.

Counting efficiencies were taken to be equal for all catchers from differential experiments. Absorption corrections were applied for integral experiments by successive approximations as follows. Range values in Au were first calculated by assuming equal counting efficiencies. Then the effective depth of the activity in the target was assumed to be the target thickness minus the range. The activity in the Al catcher foil was assumed to be distributed uniformly to a depth equal to the recoil range in Al. Each observed activity was then multiplied by $(1-d/2R_\alpha)^{-1}$, where d represents the maximum depth of the activity and R_α is the range of the α particles in the appropriate material. The R_α values were taken from decay-scheme information[13] and the range-energy data for α particles.[14] These corrections were usually less than 10% and were often nearly equal for the target and catcher foils.

III. ANALYSIS

As a starting point, we analyze the experimental results as though the recoil velocities of the nuclear-reaction products are along the beam direction. In later sections we examine the effects caused by the nuclear reaction and the stopping process. From the experimental observations we obtain the component R of the recoil range along the beam direction. We refer to R as the range. The distribution of range values, $P(R)$, is taken to be a Gaussian function,

$$P(R)dR = \frac{1}{R_0\rho(2\pi)^{\frac{1}{2}}} \exp\left[-\left(\frac{R-R_0}{\sqrt{2}R_0\rho}\right)^2\right]dR, \quad (1)$$

where R_0 is the average range, ρ is the measured straggling parameter, and $R_0\rho$ is the range straggling.
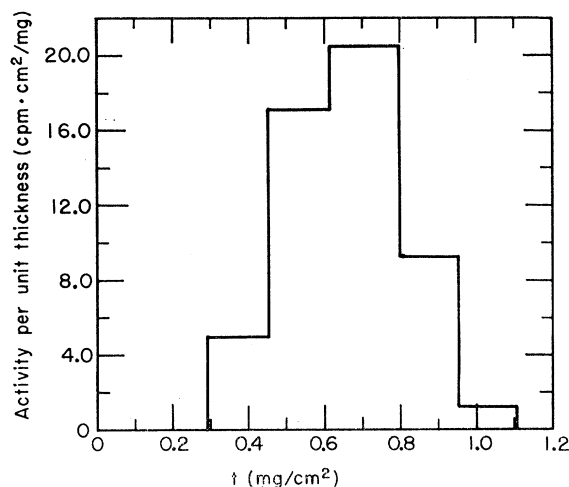
The results of the differential experiments with Al

FIG. 1. Distribution of Tb¹⁴⁹ activity in a typical differential experiment. The activity of Tb¹⁴⁹ divided by the catcher-foil thickness is plotted against total catcher-foil thickness, t. These data are from 86.8-Mev O^{16} bombardment of La. A background correction of $\approx$1.2 (counts/min cm^2/mg) has been subtracted.

[13] D. Strominger, J. M. Hollander, and G. T. Seaborg, Revs. Modern Phys. 30, No. 2 (1958).
[14] W. A. Aron, B. G. Hoffman, and F. C. Williams, U. S. Atomic Energy Commission Unclassified Document AECU–663, May 1951 (unpublished).
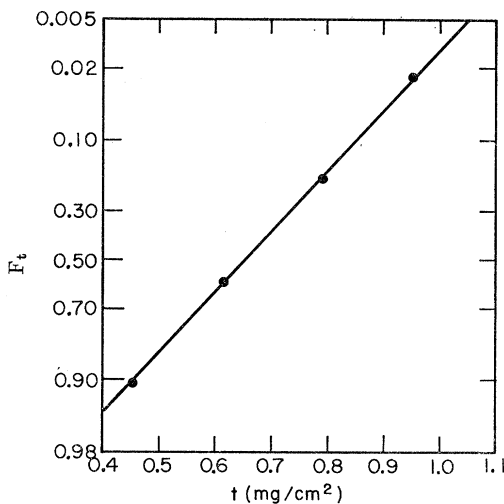
FIG. 2. Probability plot of the data shown in Fig. 1. The fraction F_t of the total activity that passed through catcher foils of combined thickness t is plotted against t.

catchers were fitted to Eq. (1) by plotting the experimental data on probability paper. On a probability scale F_t, the fraction of the total activity that passed through catcher foils of combined thickness t, was plotted against t. A very small correction for target thickness W was applied by treating the target layer as if it were an Al catcher of thickness $0.27W$. The number 0.27 is one-half the relative stopping power of Au and Al, and was used for other substances as well. This correction was always small. The t value for which $F_t = \frac{1}{2}$ specifies R_0. Similarly the t value for which $F_t = 0.0787$ gives $R_0(1+\sqrt{2}\rho)$. The results of a typical differential experiment are shown in Figs. 1 and 2. Figure 1 shows a histogram of the activity distribution, and Fig. 2 shows a probability plot of the same data.

For the integral experiments the target thickness was comparable to the recoil range. The quantity measured is the fraction F_W of the total activity formed and stopped in a target layer of thickness W. If the target thickness is several times the average range, the effect of range straggling can be ignored and we have

$$R_0 = W(1 - F_W) \qquad (2)$$

for any type of range distribution. However, a general relationship for any target thickness has been derived, based on the assumption that Eq. (1) holds for stopping in the target material. For this case the fraction of the total activity left in a target foil is

$$F_W = \frac{1}{(2\pi)^{\frac{1}{2}} R_0 W} \int_0^W \int_0^W \exp\left\{ - \left(\frac{r - s - R_0}{\sqrt{2}R_0\rho} \right)^2 \right\} dr\, ds, \qquad (3)$$

where s is the distance from the edge of the foil to the point at which the recoiling atom originates and $r-s$ is the distance it travels. The solution of this equation

can be conveniently expressed as

$$F_W = \frac{\sqrt{2}R_0\rho}{W} \left\{ F\left(\frac{R_0 - W}{\sqrt{2}R_0\rho} \right) - 2F\left(\frac{R_0}{\sqrt{2}R_0\rho} \right) \right.$$
$$\left. + F\left(\frac{R_0 + W}{\sqrt{2}R_0\rho} \right) \right\}, \qquad (4)$$

where

$$F(y) = \frac{1}{2\sqrt{\pi}} \exp(-y^2) - \frac{1}{2}[1 - I(y)]y, \qquad (5)$$

and $I(y)$ is the probability integral,

$$I(y) = \frac{2}{\sqrt{\pi}} \int_0^y \exp(-u^2) du. \qquad (6)$$

Equations (2), (3), and (4) are correct only if the rate of production of activity is constant throughout the target.

For the cases we will consider only the first term in Eq. (4) is important

$$F_W \cong \frac{\sqrt{2}R_0\rho}{W} F\left(\frac{R_0 - W}{\sqrt{2}R_0\rho} \right). \qquad (7)$$

The experimental results were analyzed by successive approximations with Eqs. (2) and (7) as follows: For a given target material and beam particle, values of R_0 as a function of bombarding energy were calculated from Eq. (2) for the experiments with rather thick targets. By use of interpolated values of R_0 and Eq. (7), values of ρ were calculated from the measurements for thinner targets. These values of ρ as a function of bombarding energy were used with Eq. (7) to get better values of R_0 and so forth.

The differential method provides more information in a single experiment than the integral method. However, some of the experimental difficulties characteristic of the differential method are avoided in an integral experiment. Both types of experiments as carried out here measure the components of the range parallel to the beam. In applications of the integral method the mass of the stopping atoms is usually comparable to or greater than the mass of the recoil atoms. Large-angle scattering is probably important in this case. Thus, the value of the range projected on the beam direction depends on scattering phenomena.

A few experiments combining the integral and differential methods have been performed. The recoil products from thick Pt targets were stopped in thin Al catchers. A quantitative analysis of these experiments requires detailed knowledge of straggling and scattering phenomena in the two materials. We therefore discuss these results only in a qualitative way.

IV. ROLE OF THE NUCLEAR-REACTION MECHANISM

The recoil properties of nuclear-reaction products give information about stopping phenomena only if the

corresponding velocities are known. The recoil velocity can be specified exactly only for a reaction at the threshold energy, E_{th}. For this situation all reaction products recoil with the velocity of the center of mass, if momentum and energy are to be conserved. In practice, experiments must be performed at bombarding energies greater than the threshold. Therefore the nature of the reaction mechanism must be known if the recoil velocities are to be calculated.

Let us examine the reaction mechanism in which an incident particle of energy E_b is absorbed to form an excited compound state. Let $\mathbf{v}$ denote the velocity of the compound nucleus, which is identical to the velocity of the center of mass. If the recoil velocity is not altered by the decay of the compound nucleus, the recoil energy E_{CN} of the final product is

$$E_{CN} = E_b A_b A_R / (A_b + A_T)^2. \tag{8}$$

The mass number is denoted by A with subscripts as follows: b the bombarding particle, R the recoil atom or final product, and T the target.

However, the recoil velocity is affected by the decay of the compound nucleus. Let us define the vector $\mathbf{V}$ as the resultant velocity of the recoil atom in the center-of-mass system. The resultant velocity in the laboratory system is $\mathbf{v}+\mathbf{V}$. Let θ denote the c.m. angle between $\mathbf{v}$ and $\mathbf{V}$ and θ_L denote the lab angle between $\mathbf{v}$ and $\mathbf{v}+\mathbf{V}$. First, we examine the effect on the recoil properties if the magnitude if $\mathbf{V}$ is unique.

The average range, R_0, measured in our experiments is the average of the projections of the distances of recoil (the linear distance from the point of origin to the final rest point) on the beam direction. In order to evaluate the dependence of R_0 on $\mathbf{v}$ and $\mathbf{V}$ one must specify how the recoil distance varies with the recoil velocity and the angular distribution of $\mathbf{V}$. We are concerned with a restricted region of values of $\mathbf{v}+\mathbf{V}$ for which it is assumed that recoil distance is equal to $k|\mathbf{v}+\mathbf{V}|^N$, where k and N are constants. The angular distribution of $\mathbf{V}$ is denoted by $W(\theta)$. Thus we have

$$R_0 = \frac{k}{2} \int_0^\pi (v^2 + V^2 + 2vV \cos\theta)^{N/2} \cos\theta_L W(\theta) \sin\theta d\theta. \tag{9}$$

For $W(\theta) = 1$ (isotropic distribution) we have

$$R_0 = \frac{kv^N}{4} \left(\frac{v}{V}\right) \left\{ \frac{(1+V/v)^{N+3} - (1-V/v)^{N+3}}{N+3} \right.$$
$$\left. + \frac{(1-V^2/v^2)}{N+1} \left[\left(1+\frac{V}{v}\right)^{N+1} - \left(1-\frac{V}{v}\right)^{N+1} \right] \right\}$$
$$= kv^N [1 + \tfrac{1}{6}(N^2+N-2)(V/v)^2 + \cdots], \tag{10}$$

and for $W(\theta)$ proportional to $1/\sin\theta$ and $v > V$ we have

$$R_0 = kv^N [1 + \tfrac{1}{4}(N^2-1)(V/v)^2 + \cdots]. \tag{11}$$

From Eqs. (10) and (11) we see that the value of R_0 is primarily determined by v for $(V/v)^2 \ll 1$. For this condition it is proper to associate the measured average range R_0 with the recoil energy given by Eq. (8). Later, we estimate $(V/v)^2$ to be ≈ 0.01. For the values of N encountered here, 1.3 to 2, this source of uncertainty in the value of R_0 is seen to be small.

We can estimate the contribution to the range straggling from the distribution of recoil velocities, $\mathbf{v}+\mathbf{V}$. The stopping process itself, as well as experimental errors, also contributes to this effect. These are considered later.

The contribution to the measured range straggling from the distribution of $\mathbf{v}+\mathbf{V}$ is given by

$$\langle (R-R_0)^2 \rangle = \frac{1}{2} \int_0^\pi [R(v,V,\theta) - R_0]^2 W(\theta) \sin\theta d\theta. \tag{12}$$

For $V/v \ll 1$ and for $W(\theta) = 1$ we have

$$\langle (R-R_0)^2 \rangle / R_0^2 = N^2 V^2 / 3v^2, \tag{13}$$

and for $W(\theta)$ proportional to $1/\sin\theta$ we have

$$\langle (R-R_0)^2 \rangle / R_0^2 = N^2 V^2 / 2v^2. \tag{14}$$

In this development the magnitude of $\mathbf{V}$ has been taken to be unique. Let us consider a distribution in magnitude of $\mathbf{V}$ with $|\mathbf{v}|$ always larger than $|\mathbf{V}|$. Then in Eqs. (10), (11), (13), and (14) the quantity V^2 is replaced by its average value, $\langle V^2 \rangle$. For $\langle V^2 \rangle / v^2 \ll 1$, Eq. (8) gives the value of the average energy to be associated with R_0. If the distribution of ranges from the effects of the nuclear reaction is a Gaussian function, with the parameter ρ_n we have

$$\rho_n^2 = \langle (R-R_0)^2 \rangle / R_0^2, \tag{15}$$

which, for the case $W(\theta) = 1$, gives

$$\rho_n^2 = N^2 \langle V^2 \rangle / 3v^2. \tag{16}$$

We can estimate the value of $\langle V^2 \rangle$ for the decay of the compound nucleus by nucleon emission in random directions in the center-of-mass system. If n nucleons are emitted, the mean square momentum of each nucleon is

$$\langle p^2 \rangle = 2[E_b A_T / (A_b + A_T) + Q]/n, \tag{17}$$

where Q is the mass difference between reactants and products. We assume here that the entire energy of excitation is removed by the nucleons. The resulting momentum of the recoiling atom in the center-of-mass system by this "random walk" process is given by

$$A_R^2 \langle V^2 \rangle = 2[E_b A_T / (A_b + A_T) + Q]. \tag{18}$$

Finally, we get

$$\langle V^2 \rangle / v^2 = [E_b A_T / (A_b + A_T) + Q]$$
$$\times (A_b + A_T)^2 / A_R^2 A_b E_b. \tag{19}$$

Actually, there is evidence that $W(\theta)$ for alpha-particle emission and fission is closer to the form $1/\sin\theta$

TABLE I. Recoil studies of Tb^{149} in Al.

Nuclear reaction	Beam energy, E_b (Mev)	Total degrader (mg/cm² Al)	Target thickness (μg/cm²)	R_0 (mg/cm² Al)	ρ	Calculated recoil energy, E_{CN} (Mev)	Calculated ρ_n
$Pr^{141}(C^{12},4n)$	55.1	45.8	33	0.367	0.28	4.21	0.09
$Pr^{141}(C^{12},4n)$	58.9	44.0	49	0.371	0.27	4.50	0.12
$Ce^{140}(N^{14},5n)$	66.0	38.9	63	0.550	0.25	5.80	0.09
$Ce^{140}(N^{14},5n)$	69.1	37.8	23	0.495	0.25	6.08	0.10
$Ce^{140}(N^{14},5n)$	73.8	36.1	63	0.545	0.25	6.49	0.12
$Ce^{140}(N^{14},5n)$	97.0	29.1	66	0.636	0.27	8.53	0.15
$Ce^{140}(N^{14},5n)$	112.1	18.9	64	0.698	0.31	9.86	0.16
$La^{139}(O^{16},6n)$	86.8	31.1	55	0.657	0.24	8.61	0.08
$La^{139}(O^{16},6n)$	95.0	28.5	12	0.730	0.23	9.43	0.10
$La^{139}(O^{16},6n)$	96.6	28.0	32	0.708	0.20	9.59	0.10
$La^{139}(O^{16},6n)$	104.4	25.4	13	0.765	0.21	10.36	0.12
$La^{139}(O^{18},8n)$	122.0	27.1	12	0.921	0.19	13.27	0.10
$Ba^{138}(Ne^{22},p10n)^a$	166.5	17.6	67	1.323	0.14	21.32	0.08
$Ba^{138}(Ne^{22},p10n)^a$	185.9	12.4	66	1.421	0.13	23.80	0.09
$Ba^{138}(Ne^{22},p10n)^a$	205.0	7.1	63	1.510	0.15	26.25	0.10
$Ba^{138}(Ne^{22},p10n)^a$	223.3	1.6	62	1.557	0.14	28.59	0.10

ᵃ The reaction $(Ne^{22},11n)$ followed by radioactive decay to form Tb^{149} is also included.

in heavy-ion bombardments.[15-17] This type of angular distribution would result in larger values of ρ_n than are given by Eq. (16). On the other hand, gamma-ray emission causes V/v to be smaller. In view of these uncertainties, we calculate ρ_n by means of Eqs. (16) and (19) with the knowledge that the resulting values are only approximate.

V. RESULTS AND DISCUSSION

A. Recoil Behavior of Tb^{149} in Al

The differential method was used to measure recoil properties of Tb^{149} in Al. A summary of the experimental results is given in Table I. In this table we include only those experiments that satisfied the following requirements: (a) decay is consistent with 4.1-hour half period; (b) range distribution is consistent with Eq. (1); (c) nuclear reactions of the type (HI,xn) or (HI,pxn); and (d) the α radioactivity observed in the most active catcher foil is at least ten times the background or activation correction. We assume that these criteria select reactions that are likely to proceed by compound-nucleus formation. The experimental results tend to justify this assumption. The experiments that do not fit these criteria are described in the following paper.[12]

The first column of Table I gives the nuclear reaction that produced Tb^{149}. The second column gives the kinetic energy, E_b, of the beam particles, as read off the range-energy curves of Northcliffe.[18] We also give the total thickness of beam-degrading foils (column 3) in terms of mg/cm² Al. For the purpose of calculating this total thickness, the target-layer thicknesses have been converted to an equivalent amount of Al by the

factor 0.535. The initial beam energy of 10.38 Mev per atomic mass unit has been measured for C^{12} by Walton.[19] We have used this figure for all ions. The target thickness, range, and straggling parameter are shown in columns 4 through 6. Column 7 gives the average recoil energy, E_{CN}, calculated from Eq. (8). The last column gives the value of ρ_n calculated from Eqs. (16) and (19).

It is clearly possible that the Tb^{149} has been produced by mechanisms other than the compound-nucleus mechanism and that Eq. (8) does not give the average energy of the recoil atoms. Therefore, we have used an extrapolation procedure to estimate the recoil range at the threshold energy, E_{th}, for the reaction. The values of the atomic masses were taken from Wapstra[20] and Cameron.[21] For $E_b = E_{th}$, Eq. (8) is (as previously discussed) independent of reaction mechanism. The ratio R_0/E_{CN} has been plotted against $E_b - E_{th}$ in Fig. 3, and a linear extrapolation to the threshold was made as shown. The resulting values of R_0 are given in Table II.

In Fig. 4 the measured and extrapolated values of R_0 are plotted against E_{CN}. A smooth curve that

TABLE II. Mean range of Tb^{149} in Al extrapolated to reaction threshold.

Nuclear reaction	E_{CN} (Mev)	R_0 (mg Al/cm²)
$Pr^{141}(C^{12},4n)$	3.83	0.33
$Ce^{140}(N^{14},5n)$	5.15	0.45
$La^{139}(O^{16},6n)$	7.52	0.61
$La^{139}(O^{18},8n)$	9.86	0.75
$Ba^{138}(Ne^{22},p10n)$	16.53	1.11

[15] W. J. Knox, A. R. Quinton, and C. E. Anderson, Phys. Rev. Letters 2, 9, 402 (1959).
[16] A. R. Quinton, H. C. Britt, W. J. Knox, and C. E. Anderson, Bull. Am. Phys. Soc. 4, 414 (1959).
[17] G. E. Gordon, A. E. Larsh, and T. Sikkeland, Phys. Rev. 118, 1610 (1960).
[18] L. C. Northcliffe, Phys. Rev. 120, 1744 (1960).

[19] John Walton, Lawrence Radiation Laboratory, University of California, Berkeley (private communication).
[20] A. H. Wapstra, Handbuch der Physik, edited by S. Flügge (Springer-Verlag, Berlin-Göttingen-Heidelberg, 1958), Vol. 38, pp. 1-37.
[21] A. G. W. Cameron, Atomic Energy of Canada Limited Report CRP-690, 1957 (unpublished).

passes through the extrapolated points is consistent with the measured points. This agreement is evidence that Eq. (8) is valid for these nuclear reactions, and hence that the Tb^{149} range-energy curve given in Fig. 4 is correct.

B. Recoil Behavior of At and Po in Al

We list in Table III our observations of At and Po recoil atoms that satisfy the following requirements: (a) range distribution is consistent with Eq. (1); (b) nuclear reactions of the types (HI,xn) or (HI,pxn); and (c) the α radioactivity observed in the most active catcher foil is at least ten times the background or activation correction. In these studies we have observed the gross α activity of the foils. In most cases the α activity was from several nuclides, as evidenced by the decay curves. We have estimated the mass number of the products from the decay properties,[13] threshold energies,[20,21] and preliminary excitation function measurements by other workers.[22] The probable mass numbers are given in the last column of Table III.

In the treatment of Tb^{149} recoil data we extrapolated the measured range values to the threshold energy and thus showed the consistency of the measurements with Eq. (8). In general, this procedure is not possible for the At and Po observations. Therefore we must assume the validity of Eq. (8) for this situation. The activity from the experiment with 72.4-Mev O^{18} ions decayed with a 1.8-hour half-period, which we assign to At^{207}. Similarly, with 70.9-Mev C^{12} ions we observed a 30-minute half-period, which we assign to At^{205}. The incident energy is only 14.0 Mev greater than the threshold for the reaction Ir^{193}(O^{18},$4n$)At^{207} in the former case, and in the latter case only 15.0 Mev greater than the threshold for Au^{197}(C^{12},$4n$)At^{205}. From the discussion of Tb^{149} recoil properties in the previous section and in the following paper, we consider it unlikely that Eq. (8) is seriously in error for bombarding energies so close
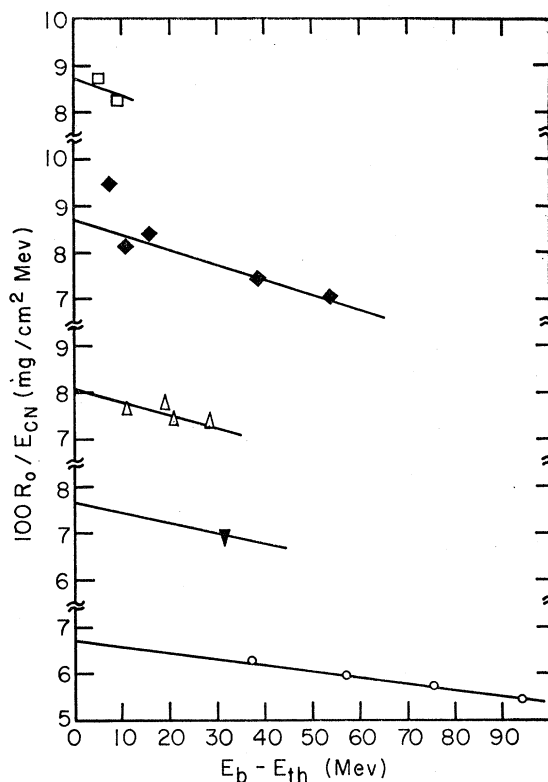

Fig. 3. Extrapolation of range data for Tb^{149} to the threshold energy. The average range is designated by R_0, the calculated recoil energy by E_{CN}, the bombarding energy by E_b, and the threshold energy by E_{th}. The points are as follows: square, bombardment by C^{12}; diamond, N^{14}; triangle, O^{16}; inverted triangle, O^{18}; circle, Ne^{22}. See Tables I and II.

to the threshold. Therefore, we have weighted these points most in drawing the range-energy curve in Fig. 4.

C. Recoil Behavior of At and Po in Au

The integral method has been used to measure the recoil properties of At and Po in Au. The recoil atoms

TABLE III. Recoil studies of At and Po in Al.

Target	Beam particle	Beam energy, E_b (Mev)	Total degrader (mg/cm²)Al	Target thickness (µg/cm²)	R_0 (mg/cm²)Al	ρ	Calculated recoil energy, E_{CN} (Mev)	Probable A_R
Au^{197}	C^{12}	70.9	37.7	44	0.281	0.28	3.99	205
Au^{197}	C^{12}	85.1	29.3	45	0.318	0.27	4.77	204
Au^{197}	C^{12}	87.7	27.6	43	0.318	0.31	4.91	204
Au^{197}	C^{12}	114.9	7.9	45	0.411	0.26	6.36	201.5
Ir	O^{18}	72.4	42.1	64	0.410	0.23	6.06	207
Ir	O^{18}	112.9	30.3	64	0.598	0.19	9.27	203
Ir	O^{18}	130.9	23.9	75	{0.670 / 0.635}	0.20 / 0.29	10.69 / 10.80	202ᵃ / 204ᵃ
Ir	O^{18}	148.1	17.2	72	0.732	0.26	12.10	202
Ir	O^{18}	164.5	10.3	78	0.770	0.24	13.37	201
Ir	O^{18}	182.9	2.0	75	0.807	0.23	14.75	199.5
Re	Ne^{22}	124.6	27.2	69	0.739	0.20	12.68	202

ᵃ Recoil properties change with time. The decay of these foils indicated the presence of two components—the half-period of about 1 hour we assign to Po^{202} and the half-period of about 4 hours we assign to Po^{204}.

[22] R. Latimer, Lawrence Radiation Laboratory (private communication, 1960).

TABLE IV. Recoil studies of At and Po in Au from C^{12} bombardment.

Beam energy, E_b (Mev)	Total degrader (mg/cm²)Al	Target thickness (mg/cm²)Au	R_0 (mg/cm²)Au	ρ	Calculated recoil energy, E_{CN} (Mev)	Estimated A_R
65.2	40.9	{0.503[a] / 0.519	0.459	0.43	3.67	205
69.8	38.4	0.643	0.503		3.93	205
79.2	33.0	2.401	0.592		4.45	204.5
83.2	30.5	0.701	0.592		4.66	204
92.1	24.6	{0.559[a] / 0.584	0.640	0.44	5.14	203
94.2	23.2	2.446	0.749		5.25	203
95.4	22.5	0.952	0.692		5.32	203
96.8	21.5	0.362		0.41	5.40	203
106.8	14.3	1.292	0.760		5.93	202
108.2	13.2	1.266	0.751		6.00	202
114.2	8.5	0.549		0.42	6.31	201
117.3	6.0	1.452	0.834		6.48	201
119.2	4.5	{0.619[a] / 0.654	0.824	0.46	6.58	201
119.6	4.2	2.45	0.881		6.60	201
119.8	3.9	1.095	0.806		6.62	201

[a] Two adjacent Au layers in the order indicated were used in these experiments. After irradiation the Au layers were peeled from the Al backing and the Au and Al samples were counted separately.

were formed by irradiation of Au targets with C^{12} and O^{16}. The experimental results for C^{12} bombardments of Au are given in Table IV. The results with O^{16} are given in Table V for the differential experiments (needed in analyzing the integral experiments) and in Table VI for the integral experiments.

We assume that Eq. (8) gives a good approximation to the recoil energy for the reactions of C^{12} with Au. This assumption is incorrect for the higher energy O^{16} bombardments. The values of E_{CN} calculated by Eq. (8) are much larger than those read off the At (in Al)

FIG. 4. Range-energy data for Tb^{149} in Al, At (and Po) in Al, and At (and Po) in Au. The points are as follows: square, bombardment by C^{12}; diamond, N^{14}; triangle, O^{16}; inverted triangle, O^{18}; circle, Ne^{22}. Closed points are measured values; open points are from extrapolation to the threshold bombarding energy. See Tables I–VII and Fig. 3.

curve in Fig. 4 for the values of R_0 given in Table V. Our measurement of the gross α activity is mainly from the decay of At and Po nuclides with some contribution possible from Em and Fr activities. These products have atomic numbers the same as, or 1 to 3 units less than, that of the compound nucleus, Fr^{213}. Thus, a variety of mechanisms, in addition to the formation of the compound nucleus, is possible. A further discussion of the mechanisms of these reactions is given in the following paper.[12]

We are unable to calculate exactly the values of recoil energies for the O^{16} experiments. However, we can associate an equivalent recoil energy, E_{eq}, with each range measurement. For this purpose we compare the measurements of the range in Al (Table V) with the range-energy curve for At in Al (Fig. 4). The energy corresponding to each range value is designated as E_{eq}. The values of E_{eq} as a function of bombarding energy are given in Table V and Fig. 5. For each of the integral range measurements in Table VI a value of E_{eq} was taken from Fig. 5. These values of E_{eq}, given in the last column of Table VI, were taken as the recoil energy
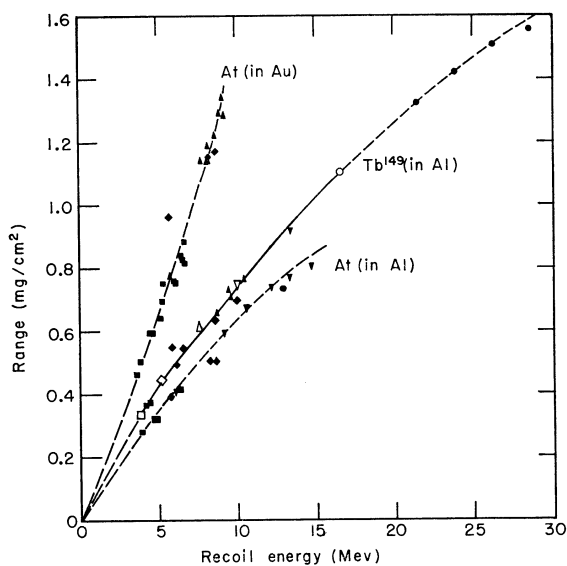
TABLE V. Recoil studies of At and Po in Al from O^{16} bombardment of Au.

Beam energy E_b (Mev)	Total degrader (mg/cm² Al)	Target thickness (μg/cm² Au)	R_0 (mg/cm² Al)	ρ	E_{eq} (Mev)
80.4	33.0	43	0.397	0.24	5.8
90.8	29.8	44	0.404	0.27	5.9
100.5	26.8	39	0.471	0.25	7.0
104.8	25.3	43	0.466	0.27	7.0
120.8	19.5	44	0.519	0.30	7.8
140.6	11.6	42	0.575	0.32	8.8
158.6	3.6	10	0.596	0.33	9.2
158.8	3.4	42	0.587	0.35	9.0

in the construction of the range-energy curve for At in Au shown in Fig. 4. We assume that the deviations of E_{eq} from the true recoil energy cancel when stopping in Al is compared to stopping in Au.

D. Range Straggling

The measured values of the straggling parameter, ρ, are given in Tables I and III to VI. The ρ values derived from the differential experiments are the results of the combination of several effects: (a) range straggling inherent in the stopping process, ρ_s; (b) velocity distribution in the nuclear reaction, ρ_n; (c) catcher-foil inhomogeneities, ρ_f; and (d) target thickness, ρ_w. The combination of these effects is given approximately as follows:

$$\rho^2 \cong \rho_s^2 + \rho_n^2 + \rho_f^2 + \rho_w^2. \tag{20}$$

The value of ρ_w can be approximated by $0.54W/2R$, the factor 0.54 being an estimate of the relative stopping power of target material and Al. The measured values of ρ are always considerably larger than ρ_w. Thus the effect of ρ_w can be subtracted quite accurately. Since we did not determine the uniformity of the foils on a microscopic scale, we have no value for ρ_f for the differential experiments. In the integral experiments ρ_w is absent in Eq. (20). We believe that the evaporated Au foils, used in the integral experiments, were uniform in thickness. Therefore ρ_f for this case is zero. Thus we get for the integral experiments

$$\rho^2 \approx \rho_s^2 + \rho_n^2. \tag{21}$$

We have already proposed a means for estimating the value of ρ_n if the nuclear reaction proceeds by way of compound-nucleus formation followed by isotropic nucleon emission [see Sec. IV and Eqs. (16) and (19)]. The values of ρ_n, calculated in this way for the Tb^{149} experiments, are given in the last column of Table I.
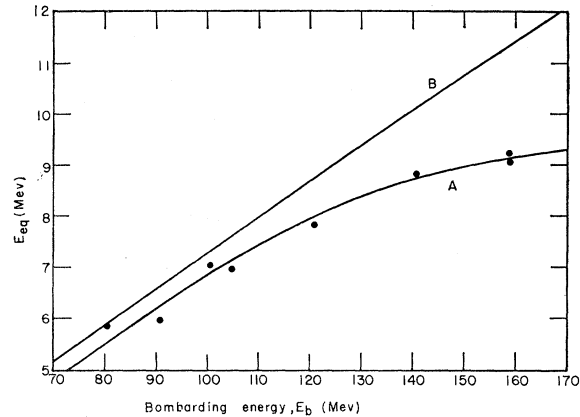

FIG. 5. E_{eq} of At and Po recoil atoms produced by O^{16} bombardment of Au as a function of the bombarding energy E_b. Curve A is a smooth curve through the experimental points. Curve B was calculated from Eq. (8); the values of A_R were estimated. The values of E_b and E_{eq} are from Table V.

The value of N at each value of the recoil energy was taken as twice the slope of the tangent to the range-energy curve as plotted on a log-log scale.

We do not expect the values of ρ_n for Tb^{149} (or for At) to be accurate. However, we do expect ρ to increase as $N\langle V^2 \rangle^{\frac{1}{2}}/v$ increases, if ρ_n is the dominant term in Eq. (20). From Table I we see that ρ is almost constant with increasing ρ_n for each given nuclear reaction. We conclude that ρ_n^2 must be small with respect to $\rho_s^2 + \rho_f^2$ for these measurements. The calculated values of ρ_n are indeed much smaller than the values of ρ (Table I). When ρ_n is much less than ρ, the crude approximations given in Eqs. (16) and (19) are adequate for subtracting the effect of ρ_n. In Fig. 6 the straggling parameters are plotted against $1/R_0$. Each point represents a measured value. An arrow has been drawn for the Tb^{149} points to indicate the magnitude of the cor-

TABLE VI. Recoil studies of At and Po in Au from O^{16} bombardment.

Beam energy, E_b (Mev)	Total degrader (mg/cm² Al)	Target thickness (mg/cm² Au)	R_0 (mg/cm² Au)	ρ	E_{eq} (Mev)
82.4	32.4	1.266	0.775		5.7
111.6	22.9	0.549		0.39	7.5
117.1	20.9	2.51	1.14		7.8
123.6	18.4	2.40	1.14		8.1
125.3	17.8	{0.695ᵃ / 1.381}	1.14	0.42	8.2
127.7	16.8	2.50	1.18		8.3
130.7	15.7	0.579		0.39	8.4
137.9	12.7	{0.950ᵃ / 1.390}	1.22	0.46	8.6
148.0	8.4	{0.934ᵃ / 1.381}	1.29ᵇ / 1.21	0.47ᵇ / 0.50	8.9
149.4	7.8	0.695		{0.41ᵇ / 0.49}	8.9
154.7	5.4	{0.961ᵃ / 1.406}	1.27	0.45ᵇ / 0.49	9.1
157.3	4.2	2.40	1.34		9.1

ᵃ Two adjacent Au layers in the order indicated were used in these experiments.
ᵇ Two values are given if a significant change in recoil properties was observed as the foils decayed. The values given here are the extremes of the observed quantities.

TABLE VII. Recoil data from N^{14} bombardment of thick Pt targets followed by thin Al foils.

Beam energy, E_b (Mev)		Total degrader (mg/cm² Al)	Target W (mg/cm² Pt)		First catcher t_1 (mg/cm² Al)		Second catcher t_2 (mg/cm² Al)			Range in Pt (mg/cm²)	Range in Al (mg/cm²)	Calculated recoil energy, E_{CN} (Mev)
Entrance	Exit			F_W		F_1		F_2	F_3			
97.7	90.3	25.9–29.3	6.33	0.849	0.127	0.0420	0.119	0.0468	0.0627	0.96	0.39	5.85[a]
135.1	130.0	6.2– 9.3	5.79	0.800	0.127	0.0375	0.131	0.0481	0.113	1.16	0.50	8.25[a]
142.7	137.5	1.6– 4.8	5.99	0.805	0.113	0.0316	0.128	0.0441	0.120	1.17	0.51	8.69[a]

[a] Based on energy of beam as it leaves target.

rection on ρ from the subtraction of ρ_n and ρ_w by means of Eq. (20).

The calculation of ρ_n for At and Po recoil atoms cannot be made accurately because of uncertainty as to the reactions observed. We estimate the value of ρ_n to be roughly 0.1 for the reactions assumed to occur by compound-nucleus formation (Table III). This crude calculation leads us to expect that the subtraction of ρ_n from ρ for At and Po stopped in Al is about the same as for Tb^{149}.

The range straggling observed for At and Po recoils in Au was always much larger than the straggling in Al. Therefore the measured straggling in Au must be mainly due to the stopping process. We estimate that ρ_s is only about 2% less than ρ for the reactions induced in Au by C^{12} (Table IV).

As noted in the preceding section, the nuclear reactions we observe in Au from the higher energy O^{16} bombardments cannot be completely attributed to a compound-nucleus mechanism. Equations (16) and (19), therefore, cannot be used for calculating ρ_n for these experiments. Instead, we have estimated ρ_n by comparing the measured ρ values from Table V (differential experiments with O^{16} and Au) with the points indicated by the tips of the arrows in the lower half of
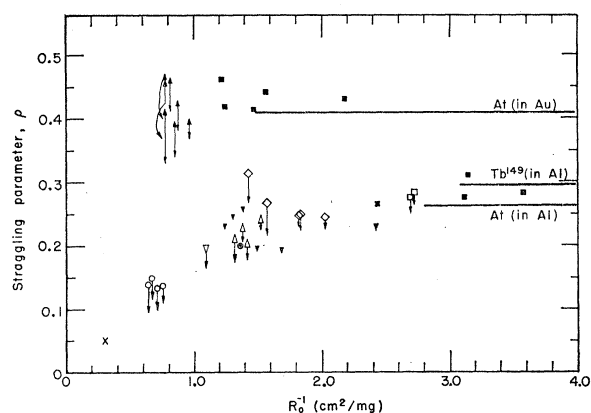

FIG. 6. Straggling parameter ρ versus the reciprocal range, R_0^{-1}. Closed points are for At (and Po); open points are for Tb^{149}; the cross is for the fission product Te^{132} [P. F. Suzor, Ann. Phys. 4, 269 (1949)]. The ρ values less than 0.32 are for stopping in Al and greater than 0.38 for stopping in Au. The symbols are as follows: square, bombardment by C^{12}; diamond, N^{14}; triangle, O^{16}; inverted triangle, O^{18}; circle, Ne^{22}. Theoretical values from Eq. (27) are shown by horizontal lines terminating at values of R_0^{-1} for which $v=v_0$.

Fig. 6. The resulting values of ρ_n were used to correct straggling measurements of At and Po in Au from O^{16} bombardment (the arrows indicated in Fig. 6).

Our method of determining ρ in the integral experiments depends on the approximation that the range distribution is of a Gaussian form. The integral method is very sensitive to the range distribution for R much less than R_0. The fact that the values of ρ are essentially constant as $(R_0-W)/R_0$ varies widely indicates that this approximation is valid (see Table IV).

E. Thick-Target Thin-Catcher Experiments

A few experiments were performed with thick Pt foils (≈ 6 mg/cm²) followed by two thin Al catchers and a thick Al catcher. In principle, this method can give values of the range in Pt and the range in Al. The results of these experiments are presented in Table VII. The first and second columns present the calculated beam energy on entrance to and exit from the target foil. In the third column is given the total Al equivalence of the degrading foils. The next seven columns give the actual experimental observations: F_W is the fraction of the total α activity observed in the target; F_1, F_2, and F_3 are the corresponding fractions observed in the three catcher foils. The thicknesses of the first two catchers are designated by t_1 and t_2. Ranges in Pt, column 11, were calculated from Eq. (2), the straggling correction being negligible. These range values may have errors due to changes in cross section because the beam energy was degraded appreciably by the target foil. An additional error may have been introduced by the large counting correction for the absorption of alpha particles in the target.

The calculation of the range in Al is not so straightforward. If the range-energy relationships in Al and Pt were proportional, and if straggling effects could be ignored, then we would have

$$R_0=\frac{(F_1+F_2+F_3)}{F_1} \qquad t_1=\frac{(F_1+F_2+F_3)}{F_2}t_2. \qquad (22)$$

This is not the case, however, as shown by values of F_i and t_i in Table VII. Those recoil atoms that spend most of their range in Pt have a broad range distribution, whereas those that lose most of their range in Al have a more narrow range distribution. Also, as shown

in Fig. 4, the range-energy relationships in Al and Pt are not simply proportional. We have not attempted to analyze these effects accurately. Instead we have made a simplifying assumption that the α activity per unit thickness increases linearly with penetration in Al to a depth equal to the range in Al. The resulting approximate values of the range in Al are given in the next-to-the-last column of Table VII. This method is subject to more uncertainty than the differential method. For this reason these measurements have been ignored in drawing the range-energy curve in Fig. 4. Nevertheless, the consistency of these results with the other data in Fig. 4 (except for the value of R_0 in Pt at 5.85 Mev) is noteworthy.

VI. COMPARISON WITH THEORY AND WITH OTHER MEASUREMENTS

Bohr's treatment of the penetration of atomic particles through matter provides a convenient framework for a discussion of our results.[1] Bohr proposes the velocity of the electron in hydrogen atom, v_0, as a rough dividing line between stopping by atomic interactions ($v < v_0$) and stopping by electronic interactions ($v > v_0$). The recoil velocities in our work extend from the vicinity of v_0 (2.2×10^8 cm/sec) to values approaching the velocities of fission fragments. It is our hope that this study of the transition region will aid in unraveling the confusing array of phenomena that contribute to the stopping process.

No theoretical treatment of the stopping process is available for the velocities that we observe. For lack of an appropriate theory we compare our results with equations derived for $v < v_0$.

The following expression has been given for $v < v_0$ and for $A_R \gg A_s$.[1,3,4]

$$R_0 = BE, \qquad (23)$$

where

$$B = 0.600 \frac{A_s(A_s + A_R)}{A_R} \frac{(Z_s^{\frac{2}{3}} + Z_R^{\frac{2}{3}})^{\frac{1}{2}}}{Z_s Z_R}. \qquad (24)$$

Here Z and A are atomic and mass numbers with subscripts s for the stopping atoms and R for the recoiling atoms. In Eqs. (23) and (24) R_0 is given in mg/cm² and E in Mev.

The experimentally determined ratio, R_0/E, from Tables I, III, IV, and VI is plotted versus E in Fig. 7. Here E refers to E_{CN} or E_{eq}. The horizontal lines with values of the ratio given by Eq. (24) extend to values of E for which the recoil velocity is $v = v_0$. The data on the stopping of Tb¹⁴⁹ and At in Al seem to be approaching the theoretical value as the recoil energy decreases.

Theoretical equations have been presented for $A_R \ll A_s$ but none for the stopping of At in Au, where $A_R \approx A_s$.[4] For $A_R \lesssim A_s$ the recoil path deviates considerably from a straight line, whereas the projection of this path on the beam direction is actually measured here. It is therefore not surprising that the values of
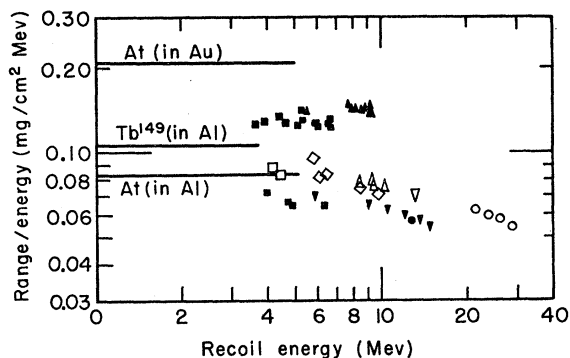

Fig. 7. Range divided by recoil energy versus recoil energy. Closed points are for At (and Po); open points for Tb¹⁴⁹. The points are as follows: square, bombardment by C¹²; diamond, N¹⁴; triangle, O¹⁶; inverted triangle, O¹⁸; circle, Ne²². The upper family of points is for stopping in Au; all other points are for stopping in Al. The lines, terminating at $v = v_0$, show the theoretical predictions from Eq. (24).

R_0/E for the stopping of At in Au (see Fig. 7) are smaller, by about 40%, than the values given by Eq. (24), compared to a 20% discrepancy for stopping in Al. The deviations from straight-line motion are expected to be smaller when Tb¹⁴⁹ and At are stopped in Al.

Our values of the range may be compared with data from several other sources for the two general cases studied here, $A_R \gg A_s$ and $A_R \approx A_s$. For the purpose of this comparison we convert the experimental results for various recoiling and stopping atoms to values for the range and energy of two "reference" systems: Xe¹³⁹ recoiling into Al, and At²⁰³ into Au. The nuclide Xe¹³⁹ represents the median-heavy fission fragment (actually $\langle Z \rangle = 53.6$, $\langle A \rangle = 138.8$) from slow-neutron fission of U²³⁵. Range-energy data are available for this case.[11]

At the same recoil velocity a given value of the average range, R_i, for an atom with atomic mass A_i recoiling into any material can be converted into the value R_0 of the reference system by the expression

$$R_0 = \frac{A_R B}{A_i B_i} R_i, \qquad (25)$$

where B and B_i are given by Eq. (24). The energy corresponding to the converted value, R_0, is, of course,

$$E = (A_R/A_i) E_i. \qquad (26)$$

The use of Eqs. (25) and (26) is justified theoretically for initial velocities less than v_0. Therefore, in the conversion to the reference system, larger errors are expected for higher initial velocities. In order to minimize the conversion errors we chose Xe¹³⁹ as the reference nuclide for the case $A_R \gg A_s$. The limits of applicability of Eqs. (25) and (26) can be tested by the experimental range data. In Fig. 8 we see that the data for Xe¹³⁹, Tb¹⁴⁹, and At²⁰³ in Al form a consistent pattern. However, if the data for the median-light fission product
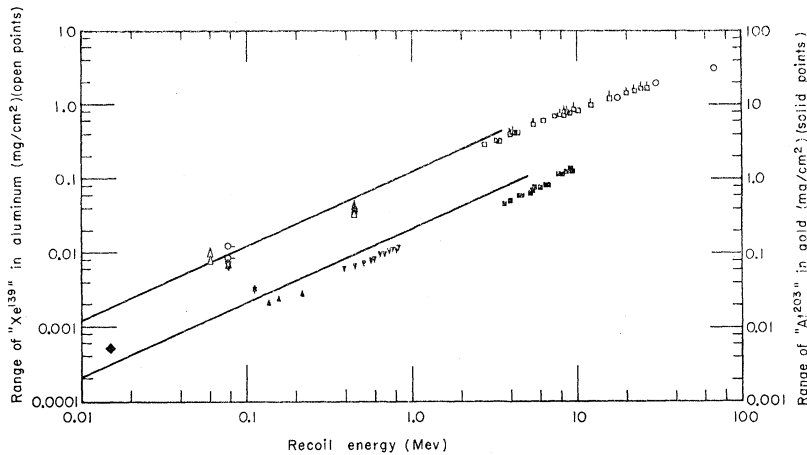
FIG. 8. Range-energy data converted to heavy fission product stopped in Al and At^{203} stopped in Au. Open points are for the heavy fission product "Xe^{139}" ($Z=53.6$, $A=138.8$) and closed points are for At^{203}. Lines terminating at $v=v_0$, are from Eqs. (23) and (24). The points are as follows: square with vertical line above it, Tb^{149}, this work; square, At^{203}, this work; circle with horizontal line beside it, reference 5; star, reference 6; triangle, reference 7; diamond, reference 9; inverted triangle, reference 10; circle, reference 11.

(Sr^{97} with recoil energy 17–98 Mev) are treated in the same way, the range values are about 25% less than the points shown in Fig. 8.

The straight lines in Fig. 8 were calculated by means of Eqs. (23) and (24) and terminate at $v=v_0$. It appears that the ratio of experimental values of the range to the calculated values is almost constant for recoil energies of about 0.1 to 10 Mev.

The values of ρ_s may be compared to an equation derived by Lindhard and Scharff,[3]

$$\rho_s = [2A_s A_R/3(A_s+A_R)^2]^{\frac{1}{2}} \qquad (27)$$

for $v<v_0$ and for $A_R \gg A_s$. The value given by Eq. (27) is shown in Fig. 6 as a horizontal line terminating at the value of R_0^{-1} for which $v=v_0$. The measured values of ρ and those calculated by Eq. (27) are nearly equal for the smaller values of R_0, even for the stopping of At in Au where $A_R \approx A_s$. One qualification must be

made for the comparison in the case of stopping in Al. After correcting for ρ_n and ρ_w, we are left with $(\rho_s^2+\rho_f^2)^{\frac{1}{2}}$. We did not measure ρ_f.

Almost all of the range straggling from the stopping process is expected to be due to atomic collisions for velocities less than v_0 and little or none from electronic interactions.[1–3] Therefore, for initial velocities greater than v_0, the range straggling, $\langle (R-R_0)^2 \rangle_s^{\frac{1}{2}}$, should be approximately constant, and ρ_s should be inversely proportional to the range. This results from the relation

$$\rho_s^2 = \langle (R-R_0)^2 \rangle_s/R_0^2. \qquad (28)$$

According to Fig. 6 this situation is approached for stopping in Al. On the other hand ρ_s should be independent of energy for initial recoil velocities less than v_0.[1,3] We can see from Fig. 6 that our measured values of ρ appear to become independent of recoil energy for low energies.